# ∞$^3$[Cu$_2$(mand)$_2$(hmt)]–MOF: A Synergetic Effect between Cu(II) and Hexamethylenetetramine in the Henry Reaction

**Horațiu Szalad [1], Natalia Candu [1], Bogdan Cojocaru [1], Traian D. Păsătoiu [2], Marius Andruh [2],* and Vasile I. Pârvulescu [1],***

[1] Department of Organic Chemistry, Biochemistry and Catalysis, Catalysis and Catalytic Processes Research Centre, Faculty of Chemistry, University of Bucharest, Bd. Regina Elisabeta nr. 4-12, 020462 Bucharest, Romania; hori.szalad@gmail.com (H.S.); natalia.candu@chimie.unibuc.ro (N.C.); bcojocaru@gmail.com (B.C.)

[2] Faculty of Chemistry, University of Bucharest, Department of Inorganic Chemistry, 23 Dumbrava Roşie Street, sector 2, 020462 Bucharest, Romania; traiandp@yahoo.com

* Correspondence: marius.andruh@dnt.ro (M.A.); vasile.parvulescu@chimie.unibuc.ro (V.I.P.)

**Abstract:** ∞$^3$[Cu$_2$(mand)$_2$(hmt)]·H$_2$O (where mand is totally deprotonated mandelic acid (racemic mixture) and hmt is hexamethylenetetramine) proved to be a stable metal–organic framework (MOF) structure under thermal activation and catalytic conditions, as confirmed by both the in situ PXRD (Powder X-ray diffraction) and ATR–FTIR (Attenuated total reflection-Fourier-transform infrared spectroscopy) haracterization. The non-activated MOF was completely inert as catalyst for the Henry reaction, as the accessibility of the substrates to the channels was completely blocked by H-bonded water to the mand entities and CO$_2$ adsorbed on the Lewis basic sites of the hmt. Heating at 140 °C removed these molecules. Only an insignificant change in the relative ratios of the XRD facets due to the capillary forces associated to the removal of the guest molecules from the network has been observed. This treatment afforded the accessibility of nitromethane and various aldehydes (4-bromobenzaldehyde, 4-nitrobenzaldehyde, and *p*-tolualdehyde) to the active catalytic sites, leading to conversions up to 48% and selectivities up to 98% for the desired nitroaldol products. The behavior of the catalyst is solvent-sensitive. Protic solvents completely inhibited the reaction due to the above-mentioned strong H-bonds. Accordingly, very good results were obtained only with aprotic solvents such as acetonitrile and 1,4-dioxane. The synthesized MOF is completely recyclable as demonstrated for five successive cycles.

**Keywords:** metal–organic frameworks; Henry reaction; heterogeneous basic catalysis; Lewis basic sites

## 1. Introduction

As catalysts, metal–organic frameworks (MOFs) are a class of materials that stand at the boundary between zeolites and enzymes. Zeolites, with surface areas around 800 m$^2$/g, can fade in comparison to MOFs when the porosity and channel regularity are taken into consideration. MOFs may provide an ultra-high porosity with some notable examples as DUT-32 [1], MOF-210 [2], or NU-100 [3]. The synthetic approach to achieve materials with such extreme values of the fraction of void volume to total volume is not complicated. An increase in the length of the organic linker could facilitate such molecular architectures [4,5], but this can also generate a decrease of the stability. On the other side, short and rigid linkers usually facilitate high thermal and chemical stability [6], and their textural properties can be tuned by branching the linking organic ligand [7,8]. Moreover, MOFs may also be designed to contain a variety of organic functional groups that decorate the channels. In a good

resemblance with enzymes, such moieties can be effective in catalysis, influencing the overall catalytic selectivity due to the steric constraints introduced by the morphology of the channels [9].

However, to be used as catalysts or adsorbents, MOFs should be firstly evacuated for the adsorbed guest molecules without any collapse of the structure [10]. To achieve such stability, the literature suggested the necessity of either $M^{+III}$ or $M^{+IV}$ nodes with a high polarizing capability [11–13] or organic linkers with high pKa values [14]. In the case of $M^{+II}$-supported MOFs, the stability may be improved by framework interpenetration [15], yet this generates a noticeable decrease in the specific surface area. In terms of catalytic activity, slight framework degradation without total collapse can be beneficial, as this may take place with the generation of defects [16]. Thus, MOFs may afford a very efficient transition from the classical homogeneous catalysis with metal complexes or from more recently organocatalysis to heterogeneous catalysis. The metallic nodes act as a backbone for the overall structure [17] but also regulate the acidity/basicity of the accessible sites [18–20].

For the specific case of the base catalyzed reactions, to date, several reports highlighted the efficient participation of the MOFs Lewis basic sites for fine organic syntheses such as the Hantzsch coupling reaction [21,22], Friedländer reaction [23], Knoevenagel condensation [24–26], aza-Michael condensation [27], or the Henry reaction [28–30]. Based on this state of the art, the aim of this study was to extend the investigation of $_{\infty}^{3}$[Cu$_2$(mand)$_2$(hmt)]·H$_2$O (where mand is totally deprotonated mandelic acid, and hmt is hexamethylenetetramine) [31] as a robust framework MOF for another important catalytic reaction, namely the Henry reaction, in the nitroaldol C–C coupling reaction, taking as substrates nitromethane and several benzaldehyde derivatives.

## 2. Materials and Methods

The reagents: copper(II) perchlorate hexahydrate (98%), mandelic acid (99%), hexamethylenetetramine (≥99%), nitromethane (≥95%), 1-nitropropane (≥98.5%), benzaldehyde (≥99%), 4-bromobenzaldehyde (99%), 4-nitrobenzaldehyde (99%), *p*-tolualdehyde (97%), 2-fluorobenzaldehyde (≥97%), and salycilaldehyde (98%) were obtained from Sigma-Aldrich (St. Louis, MI, USA) and were used without further purification. With these, the MOF catalyst has been prepared following a reported synthetic method [31]. The organic ligands have been dissolved in methanol, and the copper(II) salt has been dissolved in DMF. All the components have been mixed together in a (1:1:1) molar ratio, and the green crystals were separated after a week by filtration, washed with methanol, and air-dried. The activation of the framework has been done firstly by drying at 110 °C for 24 h and then by raising the temperature with a rate of a 1.5 °C/min until 140 °C, where it was maintained for another 24 h.
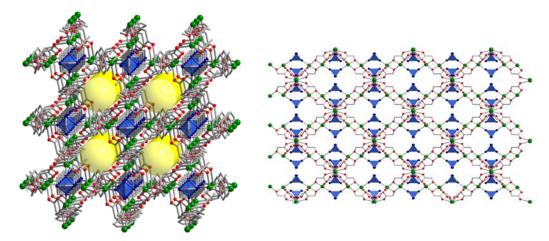
The resulted MOF has been exhaustively characterized by using TG-DTA (thermogravimetric-differential thermal analysis), PXRD, Raman, ATR–FTIR and diffuse reflectance infrared Fourier transform (DRIFT) analysis. Thermogravimetry was performed with a Shimadzu DTG-60 instrument (Kyoto, Japan) under a dry nitrogen flow (50 mL/min) with a Pt crucible. Differential thermal analysis was conducted with a Shimadzu DTA-60 instrument. Powder X-ray diffraction (XRD) patterns were recorded using a Schimadzu XRD-7000 diffractometer (Kyoto, Japan) with Cu Kα radiation (λ = 1.5418 Å, 40 kV, 40 mA) at a step of 0.2 and a scanning speed of 2 degrees per minute in the 0–60 (2θ) range. Attenuated total reflection Fourier transformed infrared spectra were recorded using a PerkinElmer Spectrum Two spectrometer having an ATR cell equipped with a diamond plate (Pike Technologies, Madison, WI, USA). The spectra were recorded with a 4 cm$^{-1}$ resolution at 20 scans. DRIFT (diffuse reflectance infrared Fourier transform) analysis was carried out using a Brucker Tensor II with a Paraying Mantis accessory. A mirror was used as reference. Raman spectra were acquired in the extended spectral region from 150 to 4000 cm$^{-1}$ using a Horiba JobinYvon-Labram HR UV-Visible-NIR Raman Microscope Spectrophotometer (Kyoto, Japan), exciting with a laser at 488 nm.

The activity tests were carried out in a glass reactor. First, 10 mg of catalyst were added to a solution of nitromethane (10 mmol), benzaldehyde derivatives (4-bromobenzaldehyde, 4-nitrobenzaldehyde

and *p*-tolualdehyde) (0.5 mmol), and 3 mL of solvent with different dielectric constants (deionized water, dried isopropyl alcohol (IPA), 1,4-dioxane, dichloromethane, dichloroethane, chloroform, or acetonitrile). The mixture has been stirred for 24 h at 50 °C. After that it has been filtered, evaporated, and then purified by a silica gel column using a mixture of petroleum ether and ethyl acetate (6:1) as eluent. Finally, the resulted solution was evaporated at room temperature, and the identification of the evolved compounds was realized with a GC-MS Carlo Erba Instruments QMD 1000 (Milan, Italy) equipped with a Factor Four VF-5HT column.

## 3. Results

Let us remind here of several structural features of the MOF under investigation [30], which are relevant for this work. $_\infty^3[Cu_2(mand)_2(hmt)]\cdot H_2O$ is a 3D coordination polymer that is constructed from binuclear alkoxido-bridged neutral nodes, $\{Cu_2(mand)_2\}$, which are connected by hmt spacers through two out of their four nitrogen atoms. The copper(II) ions show a coordination number of five, with square pyramidal geometry (Figure 1). Channels filled with water molecules, which can be easily removed, follow the crystallographic *c* axis. The two uncoordinated nitrogen atoms from the hmt spacer provide Lewis basic sites, which are of interest for catalysis.



**Figure 1.** Perspective views of $_\infty^3[Cu_2(mand)_2(hmt)]$ (the hmt molecules are drawn in blue): the channels (yellow) hosting the water molecules, which are not shown (**left**); view along the crystallographic b axis emphasizing the hmt molecules (blue) each one with two uncoordinated nitrogen atoms (**right**).

### 3.1. Characterization of the Catalysts

The structure of the fresh green MOF crystals has been checked from the recorded X-Ray diffraction pattern by comparison with the simulated one (Figure 2). The identity of the recorded positions of the diffraction lines confirmed the purity of the obtained MOF. However, the different intensity ratios of these indicated a different percentage of the different facets. A slight loss in crystallinity was measured after the thermal treatment at 140 °C for 24 h (activated MOF) (Figure 2). Such an effect has been caused by the removal of the guest molecules from the channels of the framework, which as a result has led to a minor amorphization, which is a source of beneficial defects from the catalytic point of view. However, the XRD patterns confirm that the overall crystallinity is preserved by the activated MOF with lines located in the same positions as for the fresh one.

Raising the temperature at 160 °C (Figure 3) produced an important loss of the crystallinity evidenced by the less intense lines of the facets of the MOF with a total collapse at 180 °C. XRD patterns collected at this temperature indicated the transformation of the MOF into a monoclinic $Cu_2O$ phase. Thus, lines at (2θ) 36 and 43 specific to the (110) and (111) crystalline facets of this phase clearly appeared in this pattern [32].
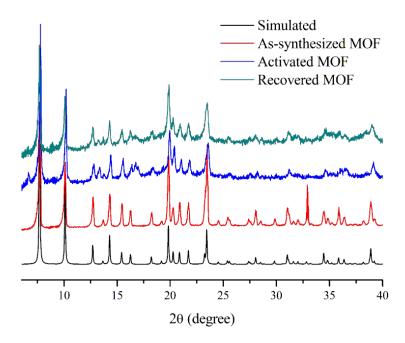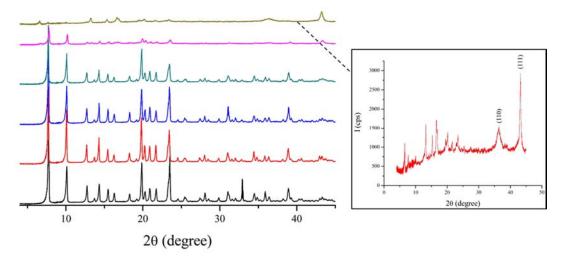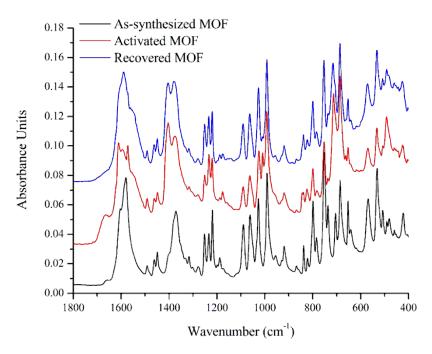
**Figure 2.** The XRD powder patterns for the simulated, as synthesized, activated, and recovered MOF.



**Figure 3.** The in-situ PXRD analysis for the metal–organic framework (MOF). The sample has been treated at 100 °C for 2 h (red line), 120 °C for 2 h (blue line), 140 °C for 2 h (green line), 160 °C for 2 h (pink line), and 180 °C for 2 h (yellow line). The black line corresponds to the simulated pattern.

To confirm the unhindered presence of the linkers in the framework of the activated MOF, comparative ATR–FTIR spectra were recorded for both the fresh and activated MOF (Figure 4). They show identical vibrations bands characteristic to the monosubstituted benzene ring at 680 cm$^{-1}$ and 790 cm$^{-1}$, to the alkoxido –O$^-$ group of the mandelic acid at 1060 cm$^{-1}$ and 1370 cm$^{-1}$, and to the carbonyl –C=O acidic bond at 1610 cm$^{-1}$. Identical bands were also detected for hexamethylenetetramine with vibrations for tertiary amino groups at ν 1220 cm$^{-1}$. For the activated and recovered MOF, the new bands at 1615, 1400, and 1000 cm$^{-1}$ are specific to the C=C and C=N in-plane vibrations (Figure 4).

Besides the in situ PXRD and ATR–FTIR, the thermal stability of the MOF has been investigated by TG–DTA. The TG–DTA analysis of the as-synthesized sample (Figure 5, left) shows that the MOF starts losing moisture at 50 °C, this weight loss being associated with an evident endothermic effect. The MOF retains its framework integrity up to 195 °C, at which temperature it rapidly collapses. The strong exothermic DTA profile of this region corresponds to the thermal decomposition of the organic ligands. The sample shows a weight loss up to 74 wt % of its original mass.

**Figure 4.** ATR–FTIR spectra of the as-synthesized MOF (black), the activated MOF (red), and the recovered MOF (blue).
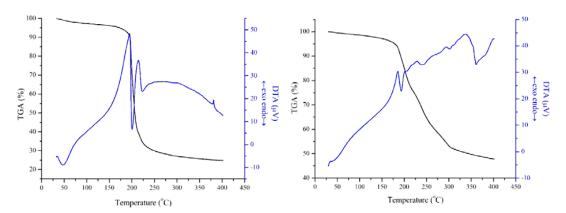


**Figure 5.** The TG–DTA profiles for the as-synthesized MOF (**left**) and the activated MOF (**right**).

The analysis done for the thermally activated sample (Figure 5, right) shows that in the first portion of the analysis, there is no weight loss associated to desolvation. A very weak signal appears on the DTA profile, which is associated with a very small amount of atmospheric water retained by the material. The activated material appears stable up to 185 °C, at which point it rapidly collapses. This sample decomposes up to 54% of its original mass, indicating that during the activation procedure, a partial decomposition of the framework takes place. Figure 5, right confirms the importance of the activation at 140 °C. Under these conditions, as both TG and DTA profiles showed, almost 20% of the mass corresponding to the molecules retained during the synthesis are removed, also affording the access of the reacting molecules during the catalytic reaction.

To investigate the nature of the slight amorphization during the thermal activation, Raman spectroscopy has been employed (Figure 6). In the case of the as-synthesized sample, the Raman lines at 998 cm$^{-1}$ and 1052 cm$^{-1}$ correspond to C–N vibrations, those at 1597 cm$^{-1}$ and 1697 cm$^{-1}$ correspond to C=O and C–N vibrations, and those at 2182 cm$^{-1}$, 2975 cm$^{-1}$, and 3056 cm$^{-1}$ correspond to the C–H vibrations [33,34]. At lower wavenumbers, the line at 256 cm$^{-1}$ is specific to Cu–O vibrations [35]. Raman spectra of the sample heated at 180 °C for 2 h does not contain any specific line of the organic linkers. However, new very intense and broad lines with maxima at 1350 to 1590 cm$^{-1}$ appeared.

These signals are specific to the D (disordered) band and G (graphitic) band specific to carbon materials. Even more, the broad line at 2800 cm$^{-1}$ is specific to the 2D band of similar materials [36]. Thus, the recorded Raman spectra suggest a minor graphitization of the material. During the solvent release, the capillary forces may break the coordination bonds, leaving behind dangling ligands. These, as they are no longer susceptive to the same polarization and network energies as the unhindered ligands, are more prone to thermal decomposition.
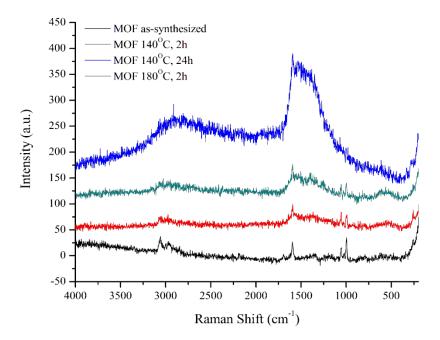


**Figure 6.** The Raman spectra recorded for MOF samples exposed to different thermal treatments.

### 3.2. Catalytic Behaviour of MOF

The investigation of the catalytic behaviour of the activated MOF has been done in several experimental steps. The first aspect considered is the solvent effect, as the interaction of these molecules with the channels will deactivate the framework by a channel fill. The ideal solvent found for this system was acetonitrile. This has been further employed in the investigation of the substituent effect upon the benzaldehyde derivatives transformation. In addition, the size capacity of the framework has been studied by the employ of 1-nitropropane as a substrate. The last aspect to be confirmed was the reaction mechanism, which has been easily confirmed via a DRIFT study.

In the absence of the catalyst, no nitroaldol reaction occurred. The carboxyl functional groups of the mandelic acid linker provide connectivity for the {Cu$_2$(mand)$_2$} binuclear nodes and the channel exposed oxygen atoms of these functionalities, which interacted with the guest molecules. Accordingly, with the protic solvents such as water or isopropanol, the framework oxygen atoms of the MOF network interact stronger as H-acceptors, hence blocking the channel. Therefore, with these solvents, the MOF did not yield any results. Interestingly enough, also no reaction products were observed when using chlorinated solvents such as chloromethane, chloroethane, or chloroform as a solvent. A possible explanation is the non-covalent interaction of these solvent molecules with the O atoms through halogen bonding [37].

The activated MOF showed a good activity for the Henry reaction with aprotic solvents (Table 1). With 1,4-dioxane, despite its very low polarity ($\varepsilon$ = 2.25), acceptable values of conversion and selectivity were obtained. The increase of the polarity of the solvent was accompanied by an increase of the conversion. The selectivity of the reaction is also solvent sensitive. Basic solvents such as acetonitrile blocked the Lewis acidity of the metal, allowing increased selectivities to nitroaldol (Table 1).

The free linkers and the metallic species have also been tested as organo- and metal catalysts (Table 2). The mandelic acid showed no activity, while with hexamethylenetetramine, the conversion of nitroalkane was of 31% and with a high selectivity to nitroalkene (96%). $Cu(ClO_4)_2 \cdot 6H_2O$ showed a higher conversion (64%) of nitro-alkane but with a selectivity to nitroaldol of only 23%, the rest being the nitroalkene. Thus, both the linker and the copper salt favorize the dehydration of nitroaldol to alkene. The fresh MOF did not show any catalytic activity.

**Table 1.** The effect of the solvent on the catalytic performance of the activated MOF (10 mmols nitromethane and 0.5 mmols benzaldehyde. 24 h 50 °C 10 mg of catalyst).



| Solvent | Conversion (%) | Selectivity for Nitroaldol (%) | Selectivity for Nitroalkene (%) |
|---|---|---|---|
| H$_2$O (deionized) | None | None | None |
| Isopropyl alcohol | None | None | None |
| Dichloromethane | None | None | None |
| Dichloroethane | None | None | None |
| Chloroform | None | None | None |
| Acetonitrile | 40 | 91 | 9 |
| 1,4-dioxane | 30 | 83 | 17 |

Turnover numbers (TONs) were calculated to compare the performances of HMT and investigated MOF by considering the participation of the nitrogens of the amine networks as the active sites. In acetonitrile, the TON of HMT was of 2.36, while for MOF, this was more than double (5.91). However, in the less polar 1,4-dioxane, the TON of MOF, although still superior to HMT, has been reduced to 4.41. This increase in activity for MOF compared to HMT might be assigned to both an effect of the Cu–N interaction and a better availability of the active sites.

*p*-Toluene-aldehyde, as the methyl substituent, exhibits an weak electron-releasing effect with no real effect on the conversion and selectivity. Accordingly, the calculated TON (5.65) and the selectivity are very close to that of the benzaldehyde. However, the other investigated aromatic substituents exhibited a very strong effect on the TON and selectivity. Thus, for the para nitro substituted substrate, the TON had a slight increase to 6.97. However, the effect was more evident for *p*-bromo-benzaldehyde which, due to the predominant resonance activated the aromatic ring, led to a considerable increase of the TON to 8.47. In addition, the probability for the formed nitroaldol to be in the proximity of a conjugated acid species $NH^+$ increases, producing an enhanced dehydration.

With 2-fluorobenzaldehyde as a substrate, the reaction followed a different pathway. Instead of the regular dehydration, both C-C coupling and elimination of the $NO_2$ functional group [38] have been evidenced. This pathway was also observed for the -Br substitued substrate, with a selectivity to the secondary product of 13%. For the much more electronegative F, the conversion was total, and the selectivity was fully shifted to the secondary product.

Salycilaldehyde was also employed as a subtrate in the Henry reaction, yet the results showed low values of conversion (12%). The reaction was also totally selective for the nitroaldol.

To investigate the size control efficiency of the synthesized MOF, a larger nitroalkane substrate has also been employed. Thus, 1-nitro-propane has been used as a substrate in the reaction with benzaldehyde under the same experimental conditions (aldehyde: nitroalkane molar ratio of 1:20, 10 mg of catalyst, 50 °C, 24 h, solvent acetonitrile). The conversion suffered a noticeable decrease to 12%, with a TON calculated value of 1.75. In addition, it is to be noted that the nitroaldol selectivity has decreased to 74%. Such a decrease in the catalytic activity can be attributed to both the morphology
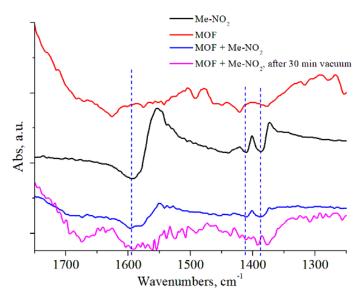
and the size of the MOF channel. The pore size of $_\infty^3[Cu_2(mand)_2(hmt)]$ is 7.9 Å [31], i.e., it is a very small value placing this MOF at the boundary between microporous and ultramicroporous materials. Another characteristic that has to be considered is the dipole-rich surface of such molecular materials, which in cotrast with the small pore size, will limit the substrate diffusion as the size of the reacting molecule increases.

**Table 2.** Catalytic results using the isolated MOF components and MOF as catalysts for the Henry reaction with various substrates (10 mmols nitromethane and 0.5 mmols benzaldehyde, 24 h, 50 °C, 10 mg of catalyst).



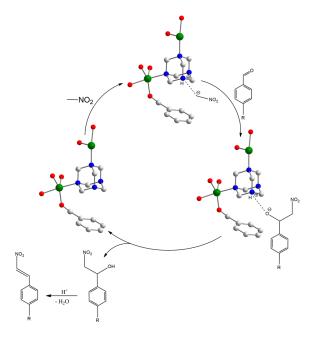| Catalyst | Solvent | Carbonyl Substrate | Conversion (%) | Selectivity for Nitroaldol (%) | Selectivity for Nitroalkene |
|---|---|---|---|---|---|
| No catalyst | 1,4-Dioxane | benzaldehyde | None | None | None |
| Mandelic Acid (5.21 mg) | Ethanol | benzaldehyde | None | None | None |
| HMT (2.4 mg) | Ethanol | benzaldehyde | 31 | 4 | 96 |
| $Cu(ClO_4)_2\cdot 6H_2O$ (12.25 mg) | Ethanol | benzaldehyde | 64 | 23 | 76 |
| Activated MOF (10 mg) | 1,4-Dioxane | benzaldehyde | 30 | 83 | 17 |
| Activated MOF (10 mg) | Acetonitrile | benzaldehyde | 40 | 91 | 9 |
| Activated MOF (10 mg) | Acetonitrile | $O_2N-$benzaldehyde | 48 | 98 | 2 |
| Activated MOF (10 mg) | Acetonitrile | $Br-$benzaldehyde | 66 | 16 | 71 |
| Activated MOF (10 mg) | Acetonitrile | F-benzaldehyde | 100 | 0 | 0 |
| Activated MOF (10 mg) | Acetonitrile | OH-benzaldehyde | 12 | 100 | 0 |
| Activated MOF (10 mg) | Acetonitrile | methyl-benzaldehyde | 39 | 89 | 11 |

To confirm the mechanism of the reaction, the catalyst was washed with the nitromethane substrate, then dried, and after that, it was analyzed by DRIFT (Figure 7). A pure nitromethane sample was used as a reference to point out its characteristic vibration bands. The signals at $\nu$ 1390, $\nu$ 1410, and 1590 cm$^{-1}$ are all characteristic to the N–O stretches. The spectra obtained from the activated MOF, as in the

ATR–FTIR analysis, show vibration bands characteristic to hexamethylenetetramine at ν 1250 and 1420 cm$^{-1}$ and mandelic acid at ν 1370 and 1620 cm$^{-1}$. Washing with the nitromethane presented in these spectra its characteristic vibration bands even after 30 min of exposure to vacuum. However, the exposure to vacuum led to a shift of the N–O stretches to lower wavenumbers, suggesting an increase in the strength of the interaction.



**Figure 7.** The diffuse reflectance infrared Fourier transform (DRIFT) spectra recorded for the nitromethane reference (black), the activated MOF (red), MOF washed by the substrate (blue), and MOF after 30 min evacuation (violet).

These results are in a good corroboration with the catalytic data, supporting the reaction mechanism described in the Figure 8.



**Figure 8.** The catalytic cycle for the Henry reaction facilitated by the MOF catalyst. The Cu$^{2+}$ atoms are illustrated in green, oxygen atoms are illustrated in red, nitrogen atoms are illustrated in blue, and carbon atoms are illustrated in gray. Hydrogen atoms have been omitted for clarity.

*3.3. The Stability of the Catalyst*

The investigated MOF has been five times recycled for the Henry coupling of benzaldehyde and p-nitro-benzaldehyde without any change in the conversion and selectivity. However, the activated MOF is moisture sensitive, and therefore, it cannot be left under atmospheric conditions for a long time. Thus, due to the adsorption of water, one week of exposure has as an effect a decrease of the conversion to only 15%, with selectivity for the nitroaldol of 56%. However, it completely recovered the initial activity after heating the sample at the same 140 °C. It is also important that the MOF preserved its crystallinity after five successive cycles.

## 4. Conclusions

The $_\infty$[Cu$_2$(mand)$_2$(hmt)]·H$_2$O MOF structure has been synthesized by assembling copper(II) ions with mandelic acid and hexamethylenetetramine in basic solution. The highly ordered channel morphology of this framework gives accessibility for two Lewis basic sites per hmt unit, while the Cu$^{2+}$ nodes are coordinatively saturated, hence not being catalytically active. This MOF offers a heterogeneous alternative to a homogenous organocatalyst. The required Lewis base active catalytic sites for the nitroaldol reaction were provided by the amino groups of the hmt linker acting as a deprotonating agent for nitromethane. However, the reaction further proceeded to nitroalkene. This step has been catalyzed by the conjugated NH$^+$ acid in situ generated during the reaction.

The synthesized MOF proved to be stable up to 140 °C. Higher temperatures induced a continuous degradation of the framework, which was evidenced by PXRD and TG–DTA weight loss, with a total collapse at 180 °C. As Raman spectroscopy showed, finally, this decomposition occurred with the formation of a graphitic material.

Non-activated MOF was completely inert from the catalytic point of view in the Henry reaction due to the blockage of the active sites by the polar molecules. However, after the thermal activation, and only with aprotic solvents, it showed an increased catalytic activity compared to HMT. Basic solvents such as acetonitrile blocked the generated Brønsted acidity, allowing increased selectivities to nitroaldol. Noteworthy, the synthesized MOF is completely recyclable. It is worth mentioning here that this MOF is assembled easily from cheap starting materials, which makes it appealing for applications.

## References

1.  Grünker, R.; Bon, V.; Müller, P.; Stoeck, U.; Krause, S.; Mueller, U.; Senkovka, I.; Kaskel, S. A new metal–organic framework with ultra-high surface area. *Chem. Commun.* **2014**, *50*, 3450–3452. [CrossRef] [PubMed]
2.  Furukawa, H.; Ko, N.; Go, Y.B.; Aratani, N.; Choi, S.B.; Choi, E.; Yazaydin, A.O.; Snurr, R.Q.; O'Keeffe, M.; Kim, J.; et al. Ultrahigh Porosity in Metal-Organic Frameworks. *Science* **2010**, *329*, 424–428. [CrossRef] [PubMed]
3.  Farha, O.K.; Yazaydin, A.O.; Eryazici, I.; Malliakas, C.D.; Hauser, B.G.; Kanatzidis, M.G.; Nguyen, S.T.; Snurr, R.Q.; Hupp, J.T. De novo synthesis of a metal–organic framework material featuring ultrahigh surface area and gas storage capacities. *Nat Chem.* **2010**, *2*, 944–948. [CrossRef] [PubMed]
4.  Yuan, D.; Zhao, D.; Sun, D.; Zhou, H.C. An Isoreticular Series of Metal–Organic Frameworks with Dendritic Hexacarboxylate Ligands and Exceptionally High Gas-Uptake Capacity. *Angew. Chem. Int. Ed.* **2010**, *49*, 5357–5361. [CrossRef] [PubMed]

5. Deng, H.; Grunder, S.; Cordova, K.E.; Valente, C.; Furukawa, H.; Hmadeh, M.; Gandara, F.; Whalley, A.C.; Liu, Z.; Asahina, S.; et al. Large-Pore Apertures in a Series of Metal-Organic Frameworks. *Science* **2012**, *336*, 1018–1023. [CrossRef]

6. Tan, Y.X.; He, Y.P.; Zhang, J. Tuning MOF Stability and Porosity via Adding Rigid Pillars. *Inorg. Chem.* **2012**, *51*, 9649–9654. [CrossRef]

7. Marx, S.; Kleist, W.; Huang, J.; Maciejewskia, M.; Baiker, A. Tuning functional sites and thermal stability of mixed-linker MOFs based on MIL-53(Al). *Dalton Tran.* **2010**, *39*, 3795–3798. [CrossRef]

8. Wittmann, T.; Siegel, R.; Reimer, N.; Milius, W.; Stock, N.; Senker, J. Enhancing the Water Stability of Al-MIL-101-NH$_2$ via Postsynthetic Modification. *Chem. Eur. J.* **2014**, *20*, 314–323.

9. Lillerud, K.P.; Olsbye, U.; Tilset, M. Designing Heterogeneous Catalysts by Incorporating Enzyme-Like Functionalities into MOFs. *Top Catal.* **2010**, *53*, 859–868. [CrossRef]

10. Mondloch, J.E.; Karagiaridi, O.; Farha, O.K.; Hupp, J.T. Activation of metal–organic framework materials. *CrystEngComm.* **2013**, *15*, 9258–9264. [CrossRef]

11. Yuan, S.; Qin, J.S.; Lollar, C.T.; Zhou, H.C. Stable Metal–Organic Frameworks with Group 4 Metals: Current Status and Trends. *ACS Cent. Sci.* **2018**, *4*, 440–450. [CrossRef] [PubMed]

12. Kang, I.J.; Khan, N.A.; Haque, E.; Jhung, S.H. Chemical and Thermal Stability of Isotypic Metal–Organic Frameworks: Effect of Metal Ions. *Chem. Eur. J.* **2011**, *17*, 6437–6442. [CrossRef] [PubMed]

13. Kandiah, M.; Nilsen, M.H.; Usseglio, S.; Jakobsen, S.; Olsbye, U.; Tilset, M.; Larabi, C.; Quadrelli, E.A.; Bonino, F.; Lillerud, K.P. Synthesis and Stability of Tagged UiO-66 Zr-MOFs. *Chem. Mater.* **2010**, *22*, 6632–6640. [CrossRef]

14. Duan, J.; Jin, W.; Kitagawa, S. Water-resistant porous coordination polymers for gas separation. *Coord. Chem. Rev.* **2017**, *332*, 48–74. [CrossRef]

15. Jasuja, H.; Walton, K.S. Effect of catenation and basicity of pillared ligands on the water stability of MOFs. *Dalton Trans.* **2013**, *42*, 15421–15426. [CrossRef]

16. Canivet, J.; Vandichel, M.; Farrusseng, D. Origin of highly active metal–organic framework catalysts: Defects? Defects! *Dalton Trans.* **2016**, *45*, 4090–4099. [CrossRef]

17. Kitagawa, S.; Kitaura, R.; Noro, S. Functional Porous Coordination Polymers. *Angew. Chem. Int. Ed.* **2004**, *43*, 2334–2375. [CrossRef]

18. Burgoyne, A.R.; Meijboom, R. Knoevenagel Condensation Reactions Catalysed by Metal-Organic Frameworks. *Catal. Lett.* **2013**, *143*, 563–571. [CrossRef]

19. Cai, J.; Wang, H.; Wang, X.; Duan, X.; Wang, Z.; Cui, Y.; Yang, Y.; Chen, B.; Qian, G. An amino-decorated NbO-type metal–organic framework for high C$_2$H$_2$ storage and selective CO$_2$ capture. *RSC Adv.* **2015**, *5*, 77417–77422. [CrossRef]

20. An, J.; Geib, S.J.; Rosi, N.L. High and Selective CO$_2$ Uptake in a Cobalt Adeninate Metal−Organic Framework Exhibiting Pyrimidine- and Amino-Decorated Pores. *J. Am. Chem. Soc.* **2010**, *132*, 38–39. [CrossRef]

21. Rostamnia, S.; Xin, H. Basic isoreticular metal–organic framework (IRMOF-3) porous nanomaterial as a suitable and green catalyst for selective unsymmetrical Hantzsch coupling reaction. *Appl. Organometal. Chem.* **2014**, *28*, 359–363. [CrossRef]

22. Rostamnia, S.; Morsali, A. Basic isoreticular nanoporous metal–organic framework for Biginelli and Hantzsch coupling: IRMOF-3 as a green and recoverable heterogeneous catalyst in solvent-free conditions. *RSC Adv.* **2014**, *4*, 10514–10518. [CrossRef]

23. Pérez-Mayoral, E.; Cejka, J. [Cu$_3$(BTC)$_2$]: A Metal–Organic Framework Catalyst for the Friedländer Reaction. *ChemCatChem.* **2011**, *3*, 157–159. [CrossRef]

24. Gascon, J.; Aktav, U.; Hernandez-Alonso, M.D.; van Klink, G.P.M.; Kapteijin, F. Amino-based metal-organic frameworks as stable, highly active basic catalysts. *J. Catal.* **2009**, *261*, 75–87. [CrossRef]

25. Valvekensa, P.; Vandichelb, M.; Waroquierb, M.; Van Speybroeck, V.; De Vos, D. Metal-dioxidoterephthalate MOFs of the MOF-74 type: Microporous basic catalysts with well-defined active sites. *J. Catal.* **2014**, *317*, 1–10. [CrossRef]

26. Luan, Y.; Qi, Y.; Gao, H.; Andriamitantsoa, R.S.; Zhenga, N.; Wang, G. A general post-synthetic modification approach of amino-tagged metal–organic frameworks to access efficient catalysts for the Knoevenagel condensation reaction. *J. Mater. Chem. A* **2015**, *3*, 17320–17331. [CrossRef]

27.  Savonnet, M.; Aguado, S.; Ravon, U.; Bazer-Bachi, D.; Lecocq, V.; Bats, N.; Pinela, C.; Farrusseng, D. Solvent free base catalysis and transesterification over basic functionalised Metal-Organic Frameworks. *Green Chem.* **2009**, *11*, 1729–1732. [CrossRef]

28.  Grupta, A.K.; Dea, D.; Bharadwaj, P.K. A NbO type Cu(II) metal–organic framework showing efficient catalytic activity in the Friedländer and Henry reactions. *Dalton Trans.* **2017**, *46*, 7782–7790. [CrossRef]

29.  Yu, H.; Xie, J.; Zhong, Y.; Zhang, F.; Zhu, W. One-pot synthesis of nitroalkenes via the Henry reaction over amino-functionalized MIL-101 catalysts. *Catal. Commun.* **2012**, *29*, 101–104. [CrossRef]

30.  Karmakar, A.; Martins, L.M.D.R.S.; Hazra, S.; da Silva, M.F.C.G.; Pombeiro, A.J.L. Metal−Organic Frameworks with Pyridyl-Based Isophthalic Acid and Their Catalytic Applications in Microwave Assisted Peroxidative Oxidation of Alcohols and Henry Reaction. *Cryst. Growth Des.* **2016**, *16*, 1837–1849. [CrossRef]

31.  Ilyes, E.; Florea, M.; Madalan, A.M.; Haiduc, I.; Parvulescu, V.I.; Andruh, M. A Robust Metal–Organic Framework Constructed from Alkoxo-Bridged Binuclear Nodes and Hexamethylenetetramine Spacers: Crystal Structure and Sorption Studies. *Inorg. Chem.* **2012**, *51*, 7954–7956. [CrossRef] [PubMed]

32.  Yang, M.; Zhu, J.J. Spherical hollow assembly composed of $Cu_2O$ nanoparticles. *J. Cryst. Growth* **2003**, *256*, 134–138. [CrossRef]

33.  Thamann, T.J.; Loehr, T.M. Raman spectra and normal coordinate analysis of the copper(II) and copper(III) complexes of biuret and oxamide. *Spectrochim. Acta A* **1980**, *36*, 751–760. [CrossRef]

34.  Dhumal, N.R.; Singh, M.P.; Anderson, J.A.; Kiefer, J.; Kim, H.J. Molecular Interactions of a Cu-Based Metal–Organic Framework with a Confined Imidazolium-Based Ionic Liquid: A Combined Density Functional Theory and Experimental Vibrational Spectroscopy Study. *J. Phys. Chem. C* **2016**, *120*, 3295–3304. [CrossRef]

35.  Escamilla-Roa, E.; Cartwright, J.H.E.; Sainz-Diaz, C.I. Chemobrionic Fabrication of Hierarchical Self-Assembling Nanostructures of Copper Oxide and Hydroxide. *ChemSystemsChem* **2019**, *1*, e190001. [CrossRef]

36.  Ferrari, A.C.; Meyer, J.C.; Scardaci, V.; Casiraghi, C.; Lazzeri, M.; Mauri, F.; Piscanec, S.; Jiang, D.; Novoselov, K.S.; Roth, S.; et al. Raman Spectrum of Graphene and Graphene Layers. *Phys. Rev. Lett.* **2006**, *97*, 187401. [CrossRef]

37.  Politzer, P.; Lane, P.; Concha, M.C.; Ma, Y.; Murray, J.S. An overview of halogen bonding. *J. Mol. Model.* **2007**, *13*, 305–311. [CrossRef]

38.  Ballini, R.; Palmieri, A. Formation of Carbon-Carbon Double Bonds: Recent Developments via Nitrous Acid Elimination (NAE) from Aliphatic Nitro Compounds. *Adv. Synth. Catal.* **2019**, *361*, 5070–5097. [CrossRef]